Manufacturing Letters 29 (2021) 113–116

Contents lists available at ScienceDirect

Manufacturing Letters

journal homepage: www.elsevier.com/locate/mfglet

Photocuring-while-writing: A 3D printing strategy to build free space structure and freeform surface texture

Jie Jin [a], Huachao Mao [b], Yong Chen [a,*]

[a] Daniel J. Epstein Department of Industrial and Systems Engineering, University of Southern California, Los Angeles, CA 90089, USA
[b] School of Engineering Technology, Purdue University, West Lafayette, IN 47907, USA

ARTICLE INFO

Article history:
Received 14 April 2021
Received in revised form 29 June 2021
Accepted 24 July 2021
Available online 30 July 2021

Keywords:
Additive manufacturing
Direct ink writing
UV-assisted
Space structure
Texture

ABSTRACT

Parts are fabricated layer-by-layer in most three-dimensional (3D) printing methods. Such a layer-based approach brings obstacles to fabricate layer-sensitive objects, such as space structures and surface textures. We present a photocuring-while-writing strategy for 3D printing. A nozzle is used to extrude photocurable material, and a laser is used to dynamically solidify the newly extruded materials instantly into desired features. Two scanning galvo mirrors control the laser spot based on a developed mathematical model. As a proof of concept, we successfully built free-standing structures and surface textures. The developed strategy may shed light on fabricating conformal features, free-standing scaffolds, and multi-material textures.

1. Introduction

Most three-dimensional (3D) printing processes are layer-based manufacturing [1–12], in which materials are added layer by layer using different energy sources and material deposition methods. By repetitively solidifying two-dimensional (2D) layers, the tool-path planning is significantly simplified. However, the layered-based fabrication methods also impose critical limitations. For example, massive support structures are required for overhanging features since the material is deposited layer by layer along the *Z*-axis direction [13]. Also, the 3D-printed parts have a rough surface quality with staircase defects, especially for the close-to-flat surfaces [14,15]. The layer-based 3D printing processes also have difficulties in printing features on freeform surfaces, such as 3D circuits [16–18] and 3D antenna [19].

Many non-layered 3D printing processes have been developed to address these limitations [20–25]. However, these non-layered-based 3D printing processes have various restrictions on resolution, accuracy, materials, etc. In this paper, we present a novel 3D printing strategy based on photocuring-while-writing (PWW) to build free space structures without supports and surface textures on a freeform surface. The printed materials considered in our study are photocurable resins or the mixture of the resins with fillers such as particles and fibers. Essentially, we integrate a scanning laser into the direct ink writing (DIW) process, and the dynamically controlled laser can instantly photocure the extrude material into desired features. Hence the PWW process is support-free and can write features on freeform surfaces, which is different from the laser-based stereolithography that uses a platform in a liquid resin tank. Also, the PWW process can work with all kinds of photocurable resins, even with the ones that have low viscosity. The printing resolution of the surface textures can be determined by the laser spot instead of the DIW process. These properties are different from the UV-assisted DIW process that uses flooded light from light emitting diodes or fixed laser diodes [26–28].

2. Material and methods

2.1. Methods

A prototype system has been built to verify the PWW process. As shown in Fig. 1a, a pneumatic extrusion system deposits liquid photocurable ink using controlled pressure. Integrated with the extrusion system in the printing head module, a 405 nm laser (Nichia NDV4512) was used to cure the ink extruded out from the nozzle tip. The laser used in the system was 250 mW, and the laser spot diameter was set between 100 μm to 300 μm. A pair of galvo mirrors dynamically adjust the position of the laser spot. The dynamic positioning control of the laser spot related to the nozzle tip is critical to ensure the PWW process to be successful.

* Corresponding author.
E-mail address: yongchen@usc.edu (Y. Chen).

https://doi.org/10.1016/j.mfglet.2021.07.016

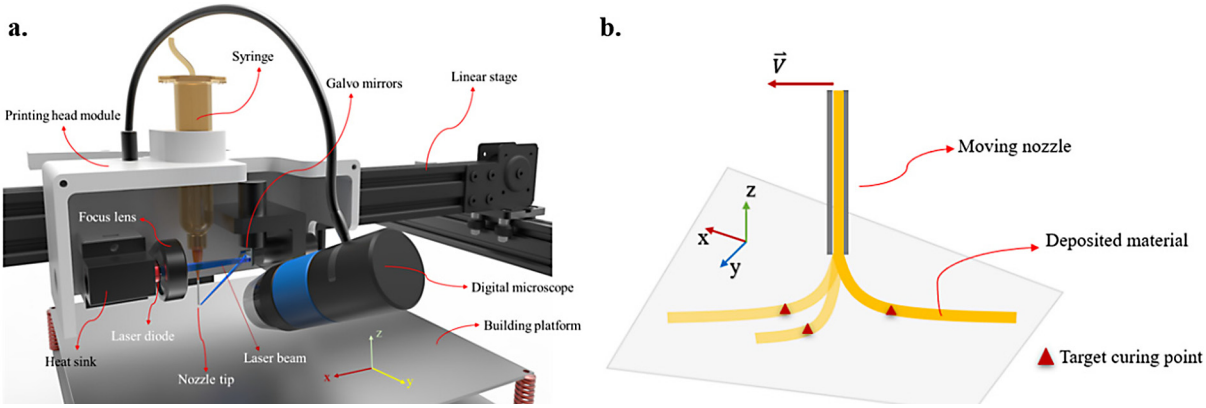

Fig. 1. Photocuring-while-writing 3D printing system. (a) The designed hardware setup of the photocuring-while-writing system; and (b) illustration of the changeable target curing point.

The galvo mirrors were controlled by a laser controller (Macpod LLC). The motion system was controlled by an open-source controller (RAMPS 1.4) with Marlin firmware embedded. A digital microscope was mounted on the printing head module to calibrate the laser system and to observe the 3D printing process in real-time.

During the translation of the printing head module, the target curing point of the newly deposited ink is not located right below the nozzle tip to avoid the photocuring of the liquid ink on the nozzle tip. Due to the changeable orientation of the extrusion traction, as shown in Fig. 1b, the position of the target curing point is associated with the moving direction of the nozzle. Thus, it is critical to dynamically track the desired target curing point for the laser spot during the extrusion process.

2.2. Material

Photocurable slurry by mixing liquid resin (40 wt% SI500 Yellow from Envision Tech.) with 60 wt% PN AP220-1 alumina powder (South Bay Tech.) was selected to build free-standing structures. Another photocurable resin (MakerJuice G+) was selected to build freeform surface textures.

3. Modeling of dynamic focusing

For an arbitrary 3D movement, the laser spot's desired position will be dynamically controlled between the center of the nozzle tip and the photocured material (refer to Fig. 2a). It is critical for the PWW process to dynamically change the laser spot's position to following the moving nozzle with a certain offset distance. Two galvo mirrors were used to navigate the laser spot dynamically and precisely. The dynamic focusing problem is to calculate the laser spot toolpath based on the liquid deposition toolpath. As shown in Fig. 2b, $\vec{D}(t)$ denotes the designed laser spot toolpath, and $\vec{S}(t)$ denotes the nozzle tip position controlled by the *XYZ* linear stage.

As shown in Fig. 2a, we first calibrate the laser spot to be exactly under the nozzle tip. We then offset the laser spot from the initial position by a certain distance to avoid the nozzle clogging. Denote the offset length L, which defines the extruded liquid ink that is currently not cured. The length L is determined by the fluid property of the liquid ink. It was set between 0.5 mm and 3 mm in our study. Hence

$$\|\vec{S}(t) - \vec{D}(t)\| = L \tag{1}$$

As shown in Fig. 2b, the position of the nozzle has the relationship with the designed tool path:

$$\vec{S}(t) = \vec{D}(t) + \frac{\nabla \vec{D}(t)}{\|\nabla \vec{D}(t)\|} \cdot r + \vec{h} \tag{2}$$

where, $\frac{\nabla \vec{D}}{\|\nabla \vec{D}\|}$ is the normalized direction of the tool path. The designed tool path $\vec{D}$ is given, and $\vec{h}$ is a constant gap between the nozzle and the curing plane to ensure successful ink extrusion.

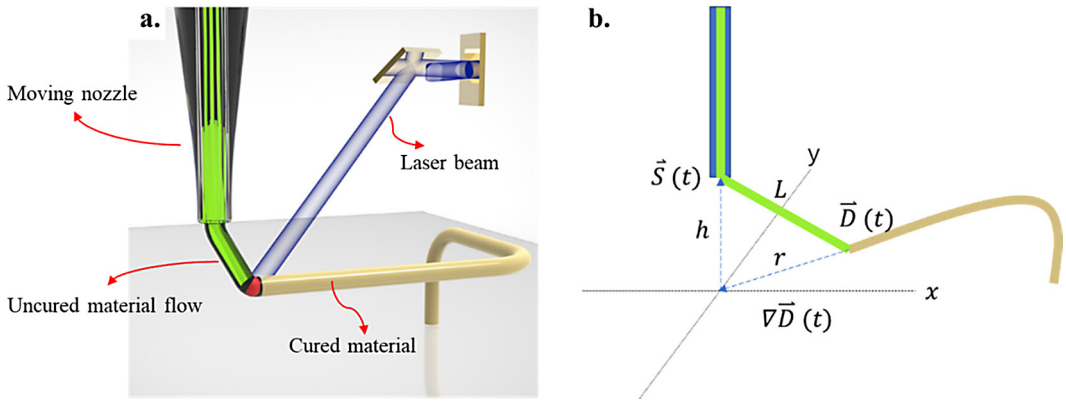

Fig. 2. A schematic drawing of the proposed dynamic focusing system.

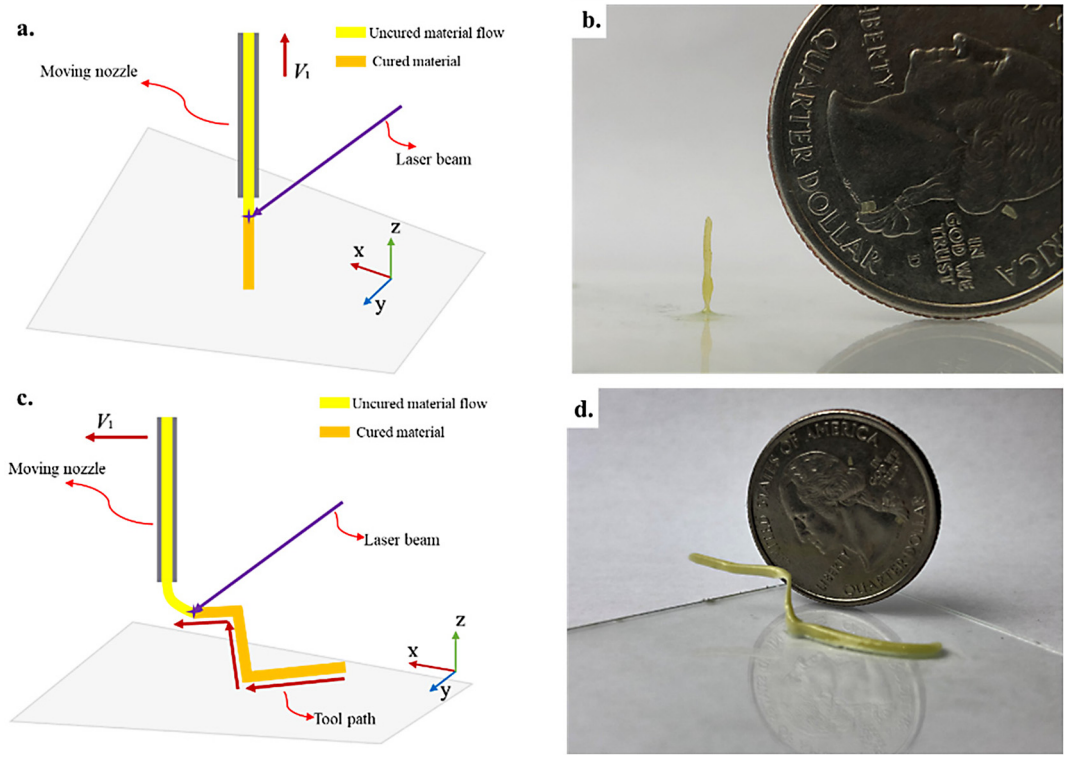

Fig. 3. Fabrication results. (a) Demonstration of printing a vertical pillar; (b) the 3D-printed result of the vertical pillar; (c) demonstration of printing a "Z" in 3D space; and (d) the 3D-printed result of the 3D "Z".

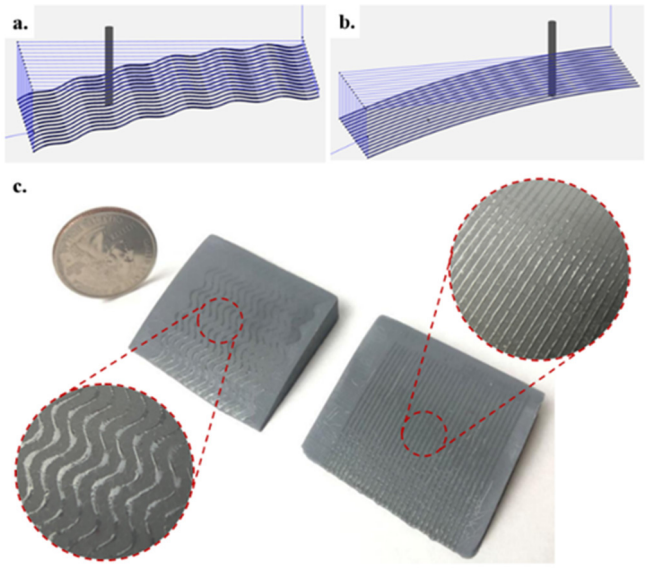

Fig. 4. Surface texture fabrication. (a) and (b) simulation of the designed toolpaths for two types of surface textures; and (c) two types of printed textures on the existing curved surfaces.

Solving the above equations yields the necessary offset distance r as

$$r = \sqrt{\left(\frac{\nabla \vec{D}(t)}{\|\nabla \vec{D}(t)\|} \cdot \vec{h}\right)^2 + L^2 - h^2} - \frac{\nabla \vec{D}(t)}{\|\nabla \vec{D}(t)\|} \cdot \vec{h} \tag{3}$$

This equation shows that the offset needs to be changed dynamically. Plugging it into equation (2) yields the paths for the ink nozzle. Note two special cases can be derived directly. The first one is when the designed tool path is moving along the XY plane, i.e., $\nabla \vec{D}(t) \cdot \vec{h} = 0$. Hence the offset distance is $r = \sqrt{L^2 - h^2}$. Another one is when the designed tool path is moving along the Z-axis, i.e., $\nabla \vec{D}(t) \times \vec{h} = 0$, and the offset distance is just $r = L - h$.

By converting the XY offset into the galvo mirror angles, we can obtain the correct laser spot dynamically. In the implementation, we used an open-source RAMPS motion controller to control the XYZ linear stage and use the LaserShark controller to control the galvo mirrors. The RAMPS controller passes the current vector $\nabla \vec{D} = (dx, dy, dz)$ to the galvo mirror controller via a personal computer in real-time and compute the offset of mirror angle to get the required $-\frac{\nabla \vec{D}}{\|\nabla \vec{D}\|} \cdot r$ offset of the laser spot in the XY plane. Considering the small angle deviation, the transformation from XY offset to mirror angle can be regarded as linear transformation:

$$\begin{bmatrix} A \\ B \end{bmatrix} = \begin{bmatrix} A_0 \\ B_0 \end{bmatrix} + \begin{bmatrix} a_{11} & a_{12} \\ a_{21} & a_{22} \end{bmatrix} \begin{bmatrix} -\frac{dx}{\sqrt{dx^2+dy^2+dz^2}} \cdot r \\ -\frac{-dy}{\sqrt{dx^2+dy^2+dz^2}} \cdot r \end{bmatrix} \tag{4}$$

In our system, the initial mirror position is $\begin{bmatrix} A_0 \\ B_0 \end{bmatrix} = \begin{bmatrix} 1860 \\ 580 \end{bmatrix}$, where the laser spot is exactly under the nozzle tip. $\begin{bmatrix} a_{11} & a_{12} \\ a_{21} & a_{22} \end{bmatrix} = \begin{bmatrix} 0 & -110 \\ 300 & 0 \end{bmatrix}$, the unit is mirror rotation step/mm. Accordingly, we can calculate the laser spot toolpath for a given shape utilizing this dynamic position compensation technique.

4. Results

4.1. Printing free-standing structures

Fig. 3a shows a printed vertical pillar to verify the PWW process. In this experiment, the nozzle diameter is 300 μm, and the lifting speed is 2 mm/s. The input constant air pressure in the syringe was set to 2 psi. The offset length L is 2 mm. The target curing point in the XY plane did not change in this experiment, and the laser spot hit on the ink trace right below the nozzle tip.

A 3D "Z" as shown in Fig. 3b was built to verify the PWW's capability of building general free-standing structures. In this case, the nozzle diameter is 600 μm, and the constant moving speed is 4 mm/s. The input constant air pressure in the syringe was set to 2 psi, and the offset length L is 2 mm. The horizontal overhanging structure was printed successfully without any supporting structures. Essentially this is a layerless DIW process for photocurable liquid resin and slurry that can be instantly solidified using a powerful laser.

4.2. Printing textures on an existing curved surface

Some surface textures, as shown in Fig. 4c were printed to demonstrate the capability of the PWW process in fabricating features on a freeform surface. In this experiment, the nozzle diameter is 200 μm, and the offset length L is 1.5 mm. Note in the traditional DIW processes, the extruded liquid resin will not stay on an inclined surface and will flow to make the extrusion resolution low. In comparison, we incorporated a laser scanning system to cure the extruded ink immediately after it comes out from the syringe tip. It ensures the dispensed material stays in the desired place, even when the target surface is curved, as shown in Fig. 4. Also, the texture feature resolution can be controlled by the laser spot size besides the extrusion process. Multimaterial surface textures can be built by incorporating additional printing head modules into the system.

5. Conclusion and discussion

A photocuring-while-writing strategy has been presented for 3D printing to build free space structures and conformal surface textures. The extruded ink is immediately photocured by a dynamically controlled laser spot behind the nozzle tip. In our study, a mathematical model was developed to control the laser spot's position with a certain offset distance. The fabrication results of some representative cases have been presented to verify PWW's capabilities in building free-standing structures and freeform surface textures. Considerable future work remains to mature the developed AM process, including (1) demonstrate multi-material printing with less material waste by integrating syringes with different liquid resins in the setup; (2) explore functional materials that are suitable for the photocuring-while-writing process and how material properties affect the PWW process; and (3) explore ultrafast laser lithography and novel applications that may benefit from the photocuring-while-writing strategy [29,30].

Declaration of Competing Interest

The authors declare that they have no known competing financial interests or personal relationships that could have appeared to influence the work reported in this paper.

References

[1] Hull, Charles W. Apparatus for production of three-dimensional objects by stereolithography. U.S. Patent 4,575,330, issued March 11, 1986.
[2] Zein I, Hutmacher DW, Tan KC, Teoh SH. Fused deposition modeling of novel scaffold architectures for tissue engineering applications. Biomaterials 2002;23(4):1169–85.
[3] Shirazi, Seyed Farid Seyed, Samira Gharehkhani, Mehdi Mehrali, Hooman Yarmand, Hendrik Simon Cornelis Metselaar, Nahrizul Adib Kadri, and Noor Azuan Abu Osman. A review on powder-based additive manufacturing for tissue engineering: selective laser sintering and inkjet 3D printing. Sci Technol Adv Mater 2015;16(3):033502.
[4] Yang, Hongyi, Jingying Charlotte Lim, Yuchan Liu, Xiaoying Qi, Yee Ling Yap, Vishwesh Dikshit, Wai Yee Yeong, Jun Wei. Performance evaluation of project multi-material jetting 3D printer. Virtual Phys Prototyping 2017;12(1):95–103.
[5] Lewis JA. Direct ink writing of 3D functional materials. Adv Funct Mater 2006;16(17):2193–204.
[6] Lewis JA, Smay JE, Stuecker J, Cesarano J. Direct ink writing of three-dimensional ceramic structures. J Am Ceram Soc 2006;89(12):3599–609.
[7] Lewis JA, Gratson GM. Direct writing in three dimensions. Mater Today 2004;7(7-8):32–9.
[8] Ahn BY, Walker SB, Slimmer SC, Russo A, Gupta A, Kranz S, et al. Planar and three-dimensional printing of conductive inks. J Visualized Experiments: JoVE 2011(58). https://doi.org/10.3791/3189.
[9] Zhou C, Chen Y, Yang Z, Khoshnevis B. Digital material fabrication using mask-image-projection-based stereolithography. Rapid Prototyping J 2013;19(3):153–65.
[10] Pan Y, Zhou C, Chen Y. A fast mask projection stereolithography process for fabricating digital models in minutes. ASME J Manuf Sci Eng 2012;134(5):051011.
[11] Pan Y, Chen Y, Yu Z. Fast mask image projection based micro-stereolithography process for complex geometry. J Micro- Nano-Manuf 2017;5(1):014501.
[12] Gu DD, Meiners W, Wissenbach K, Poprawe R. Laser additive manufacturing of metallic components: materials, processes and mechanisms. Int Mater Rev 2012;57(3):133–64.
[13] Jin J, Chen Y. Highly removable water support for Stereolithography. J Manuf Processes 2017;28:541–9.
[14] Panda, Biranchi, Suvash Chandra Paul, Nisar Ahamed Noor Mohamed, Yi Wei Daniel Tay, and Ming Jen Tan. Measurement of tensile bond strength of 3D printed geopolymer mortar. Measurement 2018;113:108–16.
[15] Willis K, Brockmeyer E, Hudson S, Poupyrev I. Printed optics: 3D printing of embedded optical elements for interactive devices. In: Proceedings of the 25th annual ACM symposium on User interface software and technology. p. 589–98.
[16] Macdonald E, Salas R, Espalin D, Perez M, Aguilera E, Muse D, et al. 3D printing for the rapid prototyping of structural electronics. IEEE Access 2014;2:234–42.
[17] Espalin D, Muse DW, MacDonald E, Wicker RB. 3D Printing multifunctionality: structures with electronics. Int J Adv Manuf Technol 2014;72(5-8):963–78.
[18] Joe Lopes A, MacDonald E, Wicker RB. Integrating stereolithography and direct print technologies for 3D structural electronics fabrication. Rapid Prototyping J 2012;18(2):129–43.
[19] Kong M, Shin G, Lee S-H, Yoon I-J. Electrically small folded spherical helix antennas using copper strips and 3D printing technology. Electron Lett 2016;52(12):994–6.
[20] Song X, Pan Y, Chen Y. Development of a low-cost parallel kinematic machine for multidirectional additive manufacturing. J Manuf Sci Eng 2015;137(2):021005.
[21] Bhatt, Prahar M, Max Peralta, Hugh A Bruck, Satyandra K Gupta. Robot assisted additive manufacturing of thin multifunctional structures. In: ASME 2018 13th International Manufacturing Science and Engineering Conference, pp. V001T01A012-V001T01A012. American Society of Mechanical Engineers; 2018.
[22] Bourell D, Chen Y, Zhou C, Lao J. A layerless additive manufacturing process based on CNC accumulation. Rapid Prototyping J 2011;17(3):218–27.
[23] Mao H, Zhou C, Chen Y. LISA: Linear immersed sweeping accumulation. J Manuf Processes 2016;24:406–15.
[24] Pan Y, Zhou C, Chen Y, Partanen J. Multitool and multi-axis computer numerically controlled accumulation for fabricating conformal features on curved surfaces. J Manuf Sci Eng 2014;136(3):031007.
[25] Highley CB, Rodell CB, Burdick JA. Direct 3D printing of shear-thinning hydrogels into self-healing hydrogels. Adv Mater 2015;27(34):5075–9.
[26] Chen K, Kuang X, Li V, Kang G, Qi J. Fabrication of tough epoxy with shape memory effects by UV-assisted direct-ink writing printing. Soft Matter 2018;14:1879–86.
[27] Vatani M, Choi J-W. Direct-print photopolymerization for 3D printing. Rapid Prototyping J 2017;23(2):337–43.
[28] Mizuno Y, Pardivala N, Tai BL. Projected UV-resin curing for self-supported 3D printing. Manuf Lett 2018;18:24–6.
[29] Malinauskas, Mangirdas, Albertas Zukauska, Satoshi Hasegawa, Yoshio Hayaysaki, Vygantas Mizeikis, Ricards Buividas, Saulius Juodkazis. Ultrafast laser processing of materials: from science to industry. Light: Sci Applications 2016;5:e16133.
[30] Ryu, Meguya, Denver Linklater, William Hart, Armandas Balcytis, Edvinas Skliutas, Mangirdas Malinauskas, Dominique Appadoo, Yaw-Ren E. Tan, Elena P Inanova, Junko Morikawa, Saulius Juodkazis. 3D printed polarizing grids for IR-THz synchrotron radiation. J Opt 2018;20:035101.